International Tables for Crystallography (2006). Vol. C, Section 2.2.6, pp. 36–37.

$$s_n = r_s \cot \bar{\nu}_n = r_s \cot \cos^{-1}(\cos \bar{\mu} - \zeta_n). \quad (2.2.5.5)$$

The resulting upper-layer photograph has outer radius

$$D(\sin \bar{\nu}_n + \sin \bar{\mu}) \quad (2.2.5.6)$$

and an inner blind region of radius

$$D(\sin \bar{\nu}_n - \sin \bar{\mu}). \quad (2.2.5.7)$$

2.2.5.5. *Recording of cone-axis photograph*

A cone-axis photograph is recorded by placing a film enclosed in a light-tight envelope in the screen holder and using a small precession angle, *e.g.* 5° for a small molecule or 1° for a protein. The photograph has the appearance of concentric circles centred on the origin of reciprocal space, provided the crystal is perfectly aligned. The radius of each circle is

$$r_n = s \tan \bar{\nu}_n, \quad (2.2.5.8)$$

where

$$\cos \bar{\nu}_n = \cos \bar{\mu} - \zeta_n. \quad (2.2.5.9)$$

Hence, $\zeta_n = \cos \bar{\mu} - \cos \tan^{-1}(r_n/s)$.

2.2.6. Diffractometry

The main book dealing with single-crystal diffractometry is that of Arndt & Willis (1966). Hamilton (1974) gives a detailed treatment of angle settings for four-circle diffractometers. For details of area-detector diffractometry, see Howard, Nielsen & Xuong (1985) and Hamlin (1985).

2.2.6.1. *General*

In this section, we describe the following related diffractometer configurations:

(*a*) normal-beam equatorial geometry [ω, χ, φ option or ω, κ, φ (kappa) option];

(*b*) fixed $\chi = 45°$ geometry with area detector.

(*a*) is used with single-counter detectors. The kappa option is also used in the television area-detector system of Enraf–Nonius (the FAST). (*b*) is used with the multiwire proportional chamber, XENTRONICS, system. (FAST is a trade name of Enraf–Nonius; XENTRONICS is a trade name of Siemens.)

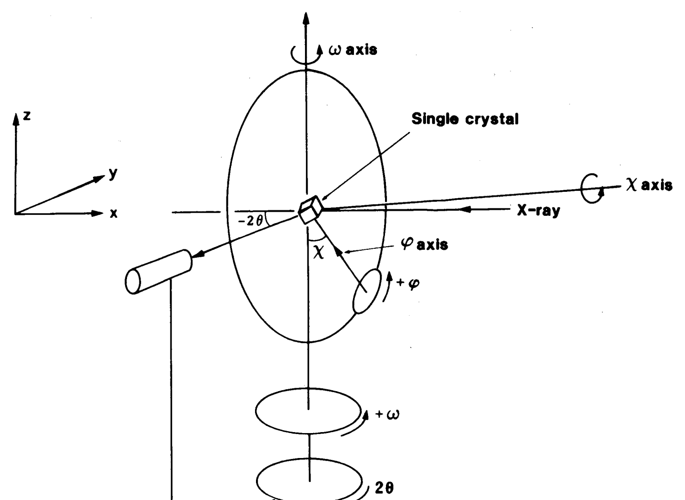

Fig. 2.2.6.1 Normal-beam equatorial geometry: the angles ω, χ, φ, 2θ are drawn in the convention of Hamilton (1974).

The purpose of the diffractometer goniostat is to bring a selected reflected beam into the detector aperture or a number of reflected beams onto an area detector of limited aperture (*i.e.* an aperture that does not intercept all the available diffraction spots at one setting of the area detector) [see Hamlin (1985, p. 431), for example].

Since the use of electronic area detectors is now increasingly common, the properties of these detectors that relate to the geometric prediction of spot position will be described later.

The single-counter diffractometer is primarily used for small-molecule crystallography. In macromolecular crystallography, many relp's are almost simultaneously in the diffraction condition. The single-counter diffractometer was extended to five separate counters [for a review, see Artymiuk & Phillips (1985)], then subsequently to a multi-element linear detector [for a review, see Wlodawer (1985)]. Area detectors offer an even larger aperture for simultaneous acquisition of reflections [Hamlin *et al.* (1981), and references therein].

Large-area on-line image-plate systems are now available commercially to crystallographers, whereby the problem of the limited aperture of electronic area detectors is circumvented and the need for a goniostat is relaxed so that a single axis of rotation can be used. Systems like the R-AXISIIc (Rigaku Corporation) and the MAR (MAR Research Systems) fall into this category, utilizing IP technology and an on-line scanner. A next generation of device beckons, involving CCD area detectors. These offer a much faster duty cycle and greater sensitivity than IP's. By tiling CCD's together, a larger-area device can be realized. However, it is likely that these will be used in conjunction with a three-axis goniostat again, except in special cases where a complete area coverage can be realized.

2.2.6.2. *Normal-beam equatorial geometry*

In normal-beam equatorial geometry (Fig. 2.2.6.1), the crystal is oriented specifically so as to bring the incident and reflected beams, for a given relp, into the equatorial plane. In this way, the detector is moved to intercept the reflected beam by a single rotation movement about a vertical axis (the 2θ axis). The value of θ is given by Bragg's law as $\sin^{-1}(d^*/2)$. In order to bring $\mathbf{d}^*$ into the equatorial plane (*i.e.* the Bragg plane into the meridional plane), suitable angular settings of a three-axis goniostat are necessary. The convention for the sign of the angles given in Fig. 2.2.6.1 is that of Hamilton (1974); his choice of sign of 2θ is adhered to despite the fact that it is left-handed, but in any case the signs of ω, χ, φ are standard right-handed. The

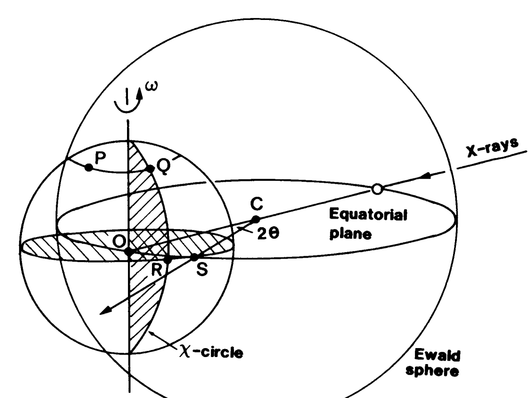

Fig. 2.2.6.2. Diffractometry with normal-beam equatorial geometry and angular motions ω, χ and φ. The relp at P is moved to Q *via* φ, from Q to R *via* χ, and R to S *via* ω. From Arndt & Willis (1966). In this specific example, the φ axis is parallel to the ω axis (*i.e.* $\chi = 0°$).

specific reciprocal-lattice point can be rotated from point *P* to point *Q* by the φ rotation, from *Q* to *R* *via* χ, and *R* to *S* *via* ω (see Fig. 2.2.6.2).

In the most commonly used setting, the χ plane bisects the incident and diffracted beams at the measuring position. Hence, the vector $\mathbf{d}^*$ lies in the χ plane at the measuring position. However, since it is possible for reflection to take place for any orientation of the reflecting plane rotated about $\mathbf{d}^*$, it is feasible therefore that $\mathbf{d}^*$ can make any arbitrary angle ε with the χ plane. It is conventional to refer to the azimuthal angle ψ of the reflecting plane as the angle of rotation about $\mathbf{d}^*$. It is possible with a ψ scan to keep the *hkl* reflection in the diffraction condition and so to measure the sample absorption surface by monitoring the variation in intensity of this reflection. This ψ scan is achieved by adjustment of the ω, χ, φ angles. When $\chi = \pm 90^\circ$, the ψ scan is simply a φ scan and ε is 0°.

The χ circle is a relatively bulky object whose thickness can inhibit the measurement of diffracted beams at high θ. Also, collision of the χ circle with the collimator or X-ray-tube housing has to be avoided. An alternative is the kappa goniostat geometry. In the kappa diffractometer [for a schematic picture, see Wyckoff (1985, p. 334)], the κ axis is inclined at 50° to the ω axis and can be rotated about the ω axis; the κ axis is an alternative to χ therefore. The φ axis is mounted on the κ axis. In this way, an unobstructed view of the sample is achieved.

2.2.6.3. *Fixed* $\chi = 45^\circ$ *geometry with area detector*

The geometry with fixed $\chi = 45^\circ$ was introduced by Nicolet and is now fairly common in the field. It consists of an ω axis, a φ axis, and χ fixed at 45°. The rotation axis is the ω axis. In this configuration, it is possible to sample a greater number of independent reflections per degree of rotation (Xuong, Nielsen, Hamlin & Anderson, 1985) because of the generally random nature of any symmetry axis.

An alternative method is to mount the crystal in a precise orientation and to use the φ axis to explore the blind region of the single rotation axis. It is feasible to place the capillary containing the sample in a vertically upright position *via* a 135° bracket mounted on the goniometer head. The bulk of the data is collected with the ω axis coincident with the capillary axis. This setting is beneficial to make the effect of capillary absorption symmetrical. At the end of this run, the blind region whose axis is coincident with the ω axis can be filled in by rotating around the φ axis by 180°. This renders the capillary axis horizontal and a different crystal axis vertical. Hence by rotation about this new crystal axis by $\pm\theta_{\max}$, the blind region can be sampled.

2.2.7. Practical realization of diffraction geometry: sources, optics, and detectors

2.2.7.1. *General*

The tools required for making the necessary measurement of reflection intensities include

(*a*) beam-conditioning items;

(*b*) crystal goniostat;

(*c*) detectors.

In this section, we describe the common configurations for defining precise states of the X-ray beam. The topic of detectors is dealt with in Part 7 (see especially Section 7.1.6). The impact of detector distortions on diffraction geometry is dealt with in Subsection 2.2.7.4.

Within the topic of beam conditioning the following subtopics are dealt with:

– collimation;
– monochromators;
– mirrors.

An exhaustive survey is not given, since a wide range of configurations is feasible. Instead, the commonest arrangements are covered. In addition, conventional X-ray sources are separated from synchrotron X-ray sources. The important difference in the treatment of the two types of source is that on the synchrotron the position and angle of the photon emission from the relativistic charged particles are correlated. One result of this, for example, is that after monochromatization of the synchrotron radiation (SR) the wavelength and angular direction of a photon are correlated.

The angular reflecting range and diffraction-spot size are determined by the physical state of the beam and the sample. *Hence, the idealized situation considered earlier of a point sample and zero-divergence beam will be relaxed.* Moreover, the effects of the detector-imaging characteristics are considered, *i.e.* obliquity, parallax, point-spread factor, and spatial distortions.

2.2.7.2. *Conventional X-ray sources: spectral character, crystal rocking curve, and spot size*

An extended discussion of instrumentation relating to conventional X-ray sources is given in Arndt & Willis (1966) and Arndt & Wonacott (1977). Witz (1969) has reviewed the use of monochromators for conventional X-ray sources.

It is generally the case that the $K\alpha$ line has been used for single-crystal data collection *via* monochromatic methods. The continuum *Bremsstrahlung* radiation is used for Laue photography at the stage of setting crystals.

The emission lines of interest consist of the $K\alpha_1$, $K\alpha_2$ doublet and the $K\beta$ line. The intrinsic spectral width of the $K\alpha_1$, or $K\alpha_2$ line is $\sim 10^{-4}$, their separation $(\delta\lambda/\lambda)$ is 2.5×10^{-3}, and they are of different relative intensity. The $K\beta$ line is eliminated either by use of a suitable metal filter or by a monochromator. A mosaic monochromator such as graphite passes the $K\alpha_1$, $K\alpha_2$ doublet in its entirety. The monochromator passes a certain, if small, component of a harmonic of the $K\alpha_1$, $K\alpha_2$ line extracted from the *Bremsstrahlung*. This latter effect only becomes important in circumstances where the *attenuated* main beam is used for calibration; the process of attenuation enhances the short-wavelength harmonic component to a significant degree. In diffraction experiments, this component is of negligible intensity. The polarization correction is different with and without a monochromator (see Chapter 6.2).

The effect of the doublet components of the $K\alpha$ emission is to cause a peak broadening at high angles. From Bragg's law, the following relationship holds for a given reflection:

$$\delta\theta = \frac{\delta\lambda}{\lambda}\tan\theta. \qquad (2.2.7.1)$$

For proteins where θ is relatively small, the effect of the $K\alpha_1$, $K\alpha_2$ separation is not significant. For small molecules, which diffract to higher resolution, this is a significant effect and has to be accounted for at high angles.

The width of the rocking curve of a crystal reflection is given by (Arndt & Willis, 1966)

$$\Delta = \left\{\left[\frac{a+f}{s}\right] + \eta + \frac{\delta\lambda}{\lambda}\tan\theta\right\} \qquad (2.2.7.2)$$

when the crystal is fully bathed by the X-ray beam, where *a* is the crystal size, *f* the X-ray tube focus size (foreshortened), *s* the